

PARTICLE ACCELERATION AS A DIAGNOSTIC FOR WAVE BRAKING IN THE SURF ZONE

Rosa Maria Vargas-Magana, University of Bergen, rosa.vargas@uib.no

Henrik Kalisch, University of Bergen, henrik.kalisch@uib.no

Maria Bjørnstad, Norwegian Meteorological Institute, mariab@met.no

Marc Buckley, Helmholtz Zentrum Hereon, marc.buckley@hereon.de

Tessa Gronemann, University of Bergen, tessa.gronemann@student.uib.no

Karoline Holand, University of Bergen, karoline.holand@student.uib.no

Jochen Horstmann, Helmholtz Zentrum Hereon, jochen.horstmann@hereon.de

Michael Stregger, Helmholtz Zentrum Hereon, michael.stresser@hereon.de

INTRODUCTION

Surf zone hydrodynamics is characterized by the dynamic interplay of various spatial and temporal scales related to different mechanical processes taking place across the surf zone. Among all the wave processes in the surf zone, wave breaking, and the associated mass transport and energy dissipation is the most significant. Wave breaking not only exerts significant forces on coastal structures but also triggers nearshore currents, and sediment transport. While our understanding of wave breaking has improved in recent decades, the precise mechanism triggering wave breaking remains unresolved.

This study focuses on utilizing the Lagrangian downward acceleration of fluid particles near the wavecrest as a dynamic criterion for identification of breaking in shallow water waves. This breaking criterion was first introduced in (Longuet-Higgins, 1963) where it was shown theoretically that the downward acceleration near the crest of a regular wave is to $-0.5g$ for breaking waves. In the subsequent literature, various other threshold values on the downward acceleration have been suggested based on theoretical or experimental investigations but a general agreement has not been established yet (Zhang et al. 2005).

Using a dedicated stereo-imaging system in a 2019 field campaign on the island of Sylt off the coast of Germany, we were able to track tracer particles during various wave conditions (Bjørnstad et al. 2021). In the present work, the data are analyzed with the goal of testing the dynamic breaking criterion.

BREAKING CRITERIA

To predict the onset of wave breaking, many criteria have been suggested, as described in (Tian et al. 2008), (Wu et al. 2002), and (Kalisch et al. 2019). There are essentially three classes of breaking criteria: Geometric, Kinematic and Dynamic criteria. While there is a resurgence of interest in the dynamic criterion in terms of wave energy flux (Derakhti et al. 2020), the literature on the criterion is related to the particle acceleration near the wave crest is rather sparse, especially for waves in shallow water. Field campaigns such as (Snyder 1983) usually focus on breaking in the open ocean, but not in the nearshore.

To assess the validity of the dynamic wave breaking criterion, we used data from a recent field campaign to test the criterion on both breaking and non-breaking waves.

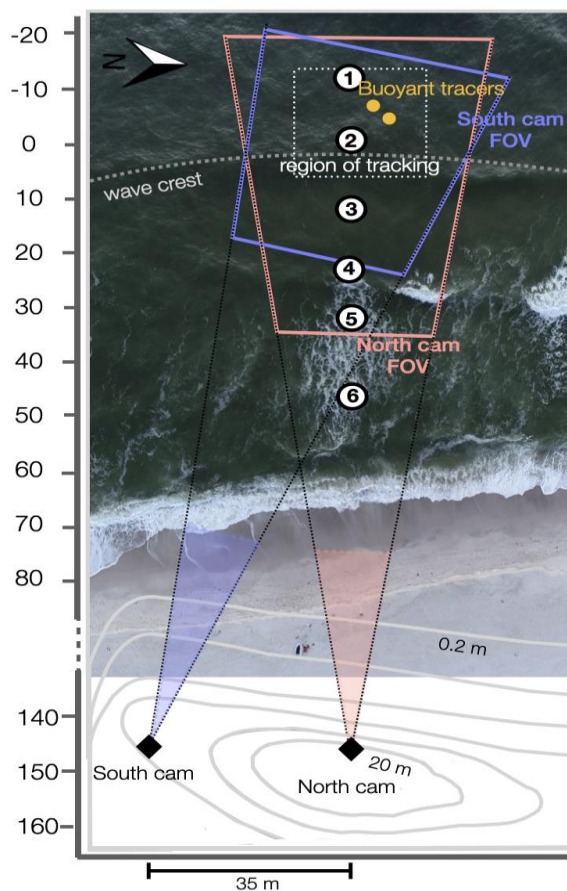


Figure 1 - Experimental Setup: Six wave staffs aligned with incoming waves, accompanied by two cameras (North cam and South cam) firmly mounted on dunes overlooking the beach.

FIELD CAMPAIGN

The field campaign was conducted on the island of Sylt, Germany, in September 2019. As part of this campaign, a vertical array of poles was strategically placed in the sediment at low tide. The array, consisting of six poles, was oriented in the direction of incoming waves. These poles were positioned at different distances from the shoreline, with Pole 1 located approximately 80 meters from the shore

and Pole 6 located 20 meters away. Pressure gauges were affixed near the seabed at these poles, and at Pole 2, an Acoustic Doppler Velocimeter (ADV) was installed in addition to the pressure gauge to measure flow velocities within the water column. In addition, a stereo imaging system was deployed. This system consisted of two cameras placed on an elevated ridge behind the beach, approximately 20 meters above sea level, and spaced 35 meters apart. The stereo imaging system featured a field of view approximately 150 meters from the camera locations. The cameras were synchronized to acquire data at a frame rate of 30 frames per second. The complete setup is shown in Figure 1.

DATA PROCESSING AND RESULTS

The main source of information in the present study are the raw images acquired by the stereo imaging system. The data analysis proceeds in four stages. First, the cameras are calibrated using special software. Once the calibration is in place, the images are examined for tracer locations, and the pixel coordinates are converted to world coordinates. After tracer trajectories are expressed in world coordinates, the paths are projected into a two-dimensional plane aligned with the pole array and the vertical direction. These steps are similar to the analysis detailed in (Bjørnstad et al. 2021). Finally, a curve-fitting procedure is applied to the two-dimensional paths in order to approximate them with a high-order polynomial using a least-square algorithm. Once the data are approximated with these high-order polynomials, the vertical acceleration can be found by evaluating the second derivative.

For these preliminary results, 23 tracer trajectories were constructed. We specifically selected trajectories in which the surface wave tracer remained visible throughout most of the recording and had sufficient path length to appreciate the wave formation and propagation. Figure 2 displays a sequence of raw images where the tracers were nicely visible. In Figure 3, we present both wave-breaking (right column) and non-breaking (left column) cases from this sample. Each plot shows the least-squares fitting curve associated with each tracer trajectory, along with the evaluation of the second derivative. A horizontal dotted line represents the threshold value of the wave-breaking criterion ($-g/2$), confirming its validity in these two cases. Out of the 23 tracer trajectories analyzed, 15 exhibited wave breaking, while 8 did not. The full results will include several hundred tracer paths.

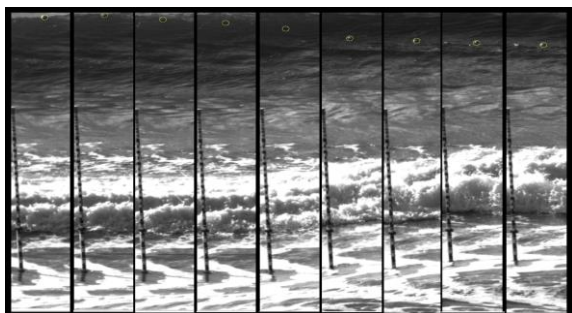


Figure 2 - Composite Image of Sequential Vertical Segments of photos Captured by the North Camera, Tracking the Buoyant Surface Tracer.

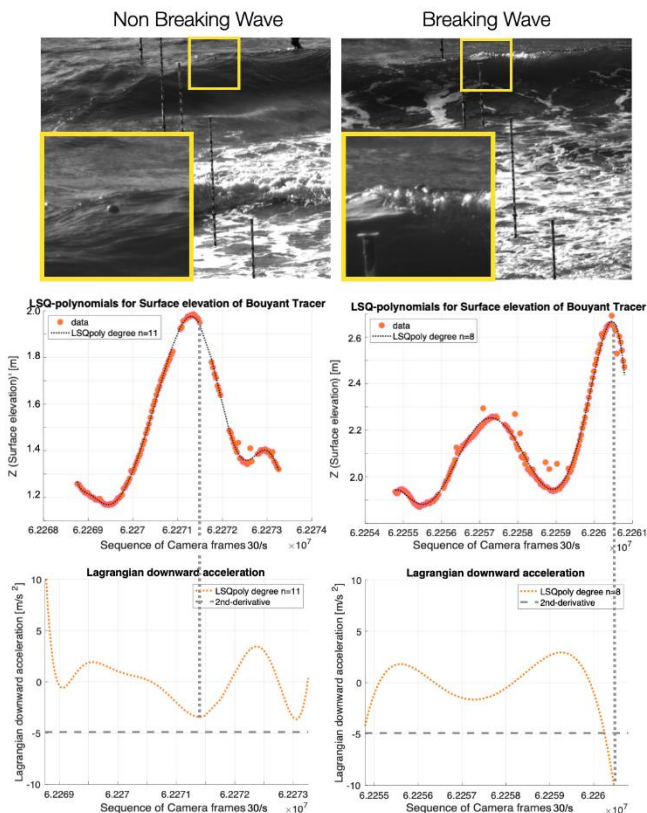


Figure 3 - Computing the Lagrangian acceleration for non-breaking (left column) and breaking (right column) waves. Upper panels: raw images. Center panels: Tracer paths and curve fit. Lower panels: Second derivative.

REFERENCES

Bjørnstad, Buckley, Kalisch, Streßer, Horstmann, Frøysa, Ige, Cysewski, Carrasco-Alvarez (2021): Lagrangian measurements of orbital velocities in the surf zone, *Geophys. Res. Letters*, vol. 48, e2021GL095722.

Derakhti, Kirby, Banner, Grilli and Thomson (2020): A unified breaking onset criterion for surface gravity water waves in arbitrary depth. *J. Geophys. Res. Oceans*, 125, e2019JC015886.

Longuet-Higgins (1963): The generation of capillary waves by steep gravity waves, *Journal of Fluid Mechanics*, vol. 16, pp.138-159.

Kalisch, Ricchiuto, Bonneton, Colin and Lubin (2019): Introduction to the special issue on breaking waves. *Eur. J. Mech. B/Fluids*, vol. 73, pp.1-5.

Snyder, Smith, Kennedy (1983): On the formation of whitecaps by a threshold mechanism. Part III: Field experiment and comparisons with theory, *J. Phys. Oceanography*, vol. 13, pp. 1505-1518.

Tian, Perlin, Choi (2008): Evaluation of a deep-water wave breaking criterion, *Phys. Fluids*, vol. 20, 066604.

Wu, Nepf (2002): Breaking criteria and energy losses for three-dimensional wave breaking, *J. Geophys. Res. Oceans*, vol. 107, 41-1.

Zhang, Yuan (2005): Energy and momentum dissipation through breaking, *J. Geophys. Res.*, vol. 110, C09021.